Bioorganic & Medicinal Chemistry 18 (2010) 8016–8025

Contents lists available at ScienceDirect

Bioorganic & Medicinal Chemistry

journal homepage: www.elsevier.com/locate/bmc

In vitro lectin-mediated selection and characterization of rHuEPO-α-binding ssDNA aptamers

Zhaoyang Zhang [a,b,†], Lei Guo [a,†], Aitao Guo [c], Hua Xu [a], Jijun Tang [a], Xingjie Guo [b], Jianwei Xie [a,*]

[a] Beijing Institute of Pharmacology and Toxicology, No. 27 Taiping Road, Beijing 100850, China
[b] School of Pharmacy, Shenyang Pharmaceutical University, No. 103 Wenhua Road, Shenhe District, Shenyang 110016, China
[c] Department of Pathology, General Hospital of the Chinese People's Liberation Army, No. 28 Fuxing Road, Beijing 100853, China

ARTICLE INFO

Article history:
Received 20 July 2010
Revised 8 September 2010
Accepted 9 September 2010
Available online 1 October 2010

Keywords:
SELEX
ssDNA aptamer
rHuEPO-α
Lectin
Immunofluorescence

ABSTRACT

A lectin-mediated affinity chromatographic SELEX technique was developed to generate functional ssDNA aptamers for recombinant human erythropoietin-α (rHuEPO-α), an important pharmaceutical glycoprotein for the first time. Secondary structure analysis of the aptamer clones from sequential 6th, 7th, and 8th rounds showed that a certain fragment 'CGAGAT' in the 3′ primer region could be used to trace increasing evolution stringency from its hybridization at different locations, in which a specific hybridization with its complement in the 5′ primer region (aptamer 807) was evolved as the prevalent one with the simplest and most common motif. Characteristics of the aptamers with lower Gibbs' free energies and K_d values (nM) were investigated. For aptamer 813, the minimer 813-42nt formed by the random and primer regions was indispensable for the specific binding with rHuEPO-α. While for aptamer 807, only the random region, that is, 807-39nt, was the functional motif. Further experiments of methylation, site-directed mutation and length variation showed that the loop of aptamer 807-39nt was the key region for binding with rHuEPO-α, and the stem should be considered as a stabilizing part. Lower cross-reactivity of aptamer 807-39nt was observed with human normal urothelium tissues than the anti-EPO monoclonal antibody AE7A5. Aptamer 807-39nt also exhibited a specific recognition for human bladder carcinoma cells and human urothelium tumors, which might provide a novel way to probe such tumors with overexpressed EPOs.

1. Introduction

Erythropoietin (EPO) is one kind of important hematopoietic growth factor, which is mainly produced in the kidney. It can regulate erythropoiesis production by activating the EPO–EPO receptor (EPOR) signaling pathway, promote the proliferation and differentiation of erythroid progenitor cells and maintain the red blood cell mass at an optimum level. EPO is a typical glycoprotein and the oligosaccharides contribute to about 40% of its molecular mass,[1] in which highly branched N-glycans stabilize the polypeptide chain consisted of many hydrophobic amino acid residues at its surface.[2]

Since 1990, a large scale of recombinant human erythropoietins (rHuEPOs) have been produced and employed extensively in clinic for anemia treatment associated with renal disease and cancer, functioning in the same way as its structure-highly-like endogenous counterpart, EPO does.[3,4] However, with a long-term administration of rHuEPOs, the accumulation of anti-EPO antibodies can raise the risk of serious anemia, blood clotting, and heart failure for the patients.[5,6]

General immunochemical or analytical methods employ antibodies as recognition molecules for rHuEPO-α,[7,8] however, antibodies now are usually generated through time-consuming procedures where animals or cell cultures are involved, and these procedures face the challenge of improving the batch-to-batch reproducibility, increasing antibodies' affinity and narrowing their specificity. While aptamers, as 'chemical antibodies', can provide a promising alternative way to obtain ligands with high affinity and high specificity for rHuEPO-α. Aptamers are generated by the technique of Systematic Evolution of Ligands by EXponential enrichment (SELEX) with a library consisting of 10^{13} to 10^{15} single-stranded (ss) nucleic acids with various random sequences,[9,10] the immense combinatorial possibilities of these sequences provide a theoretical opportunity to isolate certain RNA or DNA aptamers with excellent recognition properties for any important biomedical targets, such as metal ions, peptides, proteins, and even intact cells and tissues.[11–13]

Compared with antibodies, aptamers have a number of advantages such as stability, non-immunogenicity, resistance to denaturation, and easiness of chemical synthesis and modification.

* Corresponding author. Tel./fax: +86 10 68225893.
E-mail address: xiejw@nic.bmi.ac.cn (J. Xie).
† The authors wish it to be known that, in their opinion, the first two authors should be regarded as joint First Authors.

0968-0896/$ - see front matter © 2010 Elsevier Ltd. All rights reserved.
doi:10.1016/j.bmc.2010.09.024

Discovery of a series of anti-rHuEPO-α aptamers as a kind of effective recognition module can broaden the rHuEPO-α related researches in a certain way. Given that rHuEPO-α has large number of glycans that stretch out at the protein surface,[2] cover the peptide chain and serve as a barrier for oligonucleotides approaching, herein we introduce a promising lectin-mediated affinity chromatographic selection method to facilitate this issue, in which the N-glycans of rHuEPO-α are firstly bound to the lectin coated resin. Such an immobilization can expose the polypeptide chain and as the active binding site to the oligonucleotides (see Supplementary Scheme S1).

Several key parameters regarding to the selection procedures have been investigated in our research. After eight rounds of the selection, two aptamers named 807 and 813 with high affinity and specificity to the rHuEPO-α were isolated. The specificity and affinity of aptamer 807 were investigated in a detailed manner. The critical binding sites of aptamer 807 were studied through site-directed mutation and length variation experiments. The N-deglycosylated rHuEPO-α binding experiment further confirmed that the peptide chain was the main binding moiety for rHuEPO-α. Further immunofluorescence applications of the truncated aptamer 807-39nt on the cell and tissue-level revealed that it was comparable with anti-EPO monoclonal antibody AE7A5 in terms of binding with EPO.

2. Materials and methods

2.1. Materials

rHuEPO-α (3.89 mg/mL, purity >98.5%) was provided by SCIPROGEN Bio-pharmaceutical Co. (Shenzhen, China). ssDNA library containing a 39nt random sequence flanked by primer regions (5′-CTTCTGCCCGCCTCCTTCC-[39N]-GGAGACGAGATAGGCG GACACT-3′),[14] 6-carboxyfluorescein (FAM)-labeled forward primer (5′-CTTCTGCCCGCCTCCTTCC-3′), the biotinylated reverse primer (5′-AGTGTCCGCCTATCTCGTCTCC-3′), and other ssDNA sequences were synthesized by Shanghai Sangon Biological Engineering Technology & Services Company (Shanghai, China). Monoclonal anti-EPO antibody (clone AE7A5, purified mouse IgG2a) was purchased from R&D Systems Inc. (Minneapolis, MN, USA). Fluorescein isothiocyanate (FITC)-conjugated goat anti-mouse IgG and tetramethylrhodamine isothiocyanate (TRITC)-conjugated goat anti-mouse IgG were purchased from Jackson ImmunoResearch Laboratories Inc. (West Grove, PA, USA). Wheat germ agglutinin (WGA)-Sepharose, *N*-acetyl-D-glucosamine and PNGase F (proteomics grade) were supplied by Sigma Aldrich Inc. (St. Louis, MO, USA). The human bladder carcinoma cell line T24 and the human lens epithelial cell line HLE-B3 (from ATCC) were cultured in DMEM and in McCoy's 5A medium, respectively, supplemented with 10% fetal bovine serum. The paraffin embedded slides of human normal and tumor urothelium were kindly provided by the General Hospital of the Chinese People's Liberation Army. All other reagents were of analytical purity and obtained from Sinopharm Chemical Reagent Beijing Co., Ltd (Beijing, China). Deionized and pyrogen-free water was obtained from a Milli-Q water purification system (Millipore, MA, USA).

2.2. PCR amplification and preparation of ssDNA

The enriched ssDNA library was firstly amplified by symmetric PCR. FAM-labeled forward primer and biotinylated reverse primer were used in PCR amplification (5 min at 94 °C, then 30 s at 94 °C, 15 s at 56 °C, and 15 s at 72 °C as the cycle, followed by 5 min at 72 °C). Different PCR cycles were adopted depending on the concentration of the template. The PCR products were added to the streptavidin-coated paramagnetic beads (STV-MBs, Promega, WI, USA) and mixed at 37 °C for 6 h on a shaking platform, then the beads were washed with sodium chloride–sodium citrate buffer (SSC, pH 7.0) for three times. Three hundred microliters of 0.15 mol/L NaOH was applied onto STV-MBs to facilitate the dissociation of ssDNAs from their biotinylated complementary sequences for 1.5 min at room temperature. The supernatant was then moved to another vial containing 30 μL of 10% acetic acid solution, followed by adding 1 mL acetone and 30 μL of 22% lithium perchlorate ($LiClO_4$) to precipitate the ssDNA library.

2.3. In vitro selection of aptamers for rHuEPO-α

The selection buffer consisted of 20 mM Tris, 140 mM NaCl, 5 mM $MgCl_2$, and 5 mM KCl (pH 7.4). After 100 μL WGA-Sepharose being suspended in 220 μL selection buffer, 2000 pmol rHuEPO-α was added into the buffer and incubated for 4 h, then the rHuEPO-α-WGA-Sepharose was washed with selection buffer and stored at 4 °C for the next step. In each round, the ssDNA library in 300 μL selection buffer was denatured at 94 °C for 5 min and immediately placed on ice for 10 min.

In the beginning of the first round, the native library was subjected to a negative selection with blank Sepharose. Four micromolar tRNA was added to the incubation mixture containing library and rHuEPO-α-WGA-Sepharose in each selection round to suppress non-specific nucleic acid–protein interaction. Elution buffer (0.45 M *N*-acetyl-D-glucosamine) was added to replace the ssDNA–rHuEPO-α complex from the WGA-Sepharose, and then the eluent was mixed with 1:1 (v/v) phenol–chloroform solution and centrifuged at 14,000*g* for 10 min. The supernatant was mixed with 1 mL acetone and 30 μL of 22% $LiClO_4$ to precipitate the oligonucleotide library at −20 °C overnight. The combination of acetone and $LiClO_4$ employed here can effectively precipitate more ssDNAs of short lengths in comparison with ethanol-based method.[15] After centrifugation, the sediment was dissolved in 50 μL sterile water as the template for the next round selection. The concentrations of target and library used in selection process are summarized in Supplementary Table S1.

After eight rounds of selection, the enriched 6th, 7th, and 8th libraries were amplified by symmetry PCR with non-labeled primers. After being purified by 10% non-denatured polyacrylamide gel (PAGE), the PCR product was subsequently cloned using the plasmid pGEM-T (Promega) and transferred into *Escherichia coli* DH5α. Positive clones were randomly picked out and grown in Lurib-Bertani medium containing 100 μg/mL ampicillin, and the plasmids from individual bacterial clones were sequenced in Invitrogen Biotechnology Company using 3730 DNA sequence Analyzer (Applied Biosystems, USA).

2.4. The binding percentage and affinity of the ssDNA library

Native or enriched FAM-labeled library in each round was adopted to assess the enrichment efficiency. Hundred microliters of WGA-Sepharose beads suspended solution with or without 500 pmol rHuEPO-α was incubated with FAM-labeled libraries (100 pmol) of each round at 37 °C for 1 h in 200 μL selection buffer. After removing unspecific oligonucleotides by washing the rHuEPO-α-WGA-Sepharose three times with selection buffer, the binding oligonucleotides were eluted with elution buffer twice. The fluorescence intensity (FI) of the eluent was measured on a HITACHI F4010 spectrofluorometer, with an excitation at 494 nm and an emission at 526 nm, respectively. The slit widths for both emission and excitation were set at 5 nm.

Native library, 4th, 6th, 7th, and 8th libraries were applied in electrophoretic mobility shift assay (EMSA) to evaluate the binding percentage between library and rHuEPO-α. Each DNA library was

end-labeled with 20 μCi [γ-^{32}P] ATP by T4 Polynucleotide Kinase (TaKaRa). Twenty-five nanomolar γ-^{32}P-labeled DNA library was incubated with 1 μM rHuEPO-α in selection buffer for 1 h at 37 °C. Electrophoresis was performed on 12% non-denatured PAGE at 22 V/cm for 1 h at 4 °C. The gel was exposed to X-ray film at −20 °C overnight, and then visualized by autoradiography. Radioactivity of individual bands was analyzed by UVP VisionWorks™LS Image Software (UVP, USA).

2.5. The affinity and specificity of aptamers

To evaluate the K_d values between aptamers and target protein, EMSA method was adopted. Twenty-five nanomolar γ-^{32}P-aptamers (807, 807-68nt, 807-39nt, 813, and 850) were incubated with increasing concentration of protein (0–1500 nM) at 37 °C for 1 h, then applied in the 12% non-denatured PAGE. To calculate the K_d values, the ratio of bound ssDNA/total ssDNA (y) versus rHuEPO-α concentration (x) was plotted, and the data were fitted by the non-linear regression analysis in Origin 7.5 (OriginLab, USA) using one-site binding model: $y = B_{max}x/(K_d + x)$, where B_{max} is the degree of saturation and K_d is the dissociation constant.

The specificity of aptamer 807 was also evaluated by EMSA. Twenty-five nanomolar γ-^{32}P-labeled aptamer 807 was incubated with different proteins (1500 nM) in selection buffer for 1 h at 37 °C, and the electrophoresis was performed as above.

The binding ability of a series of different truncated aptamers derived from aptamer 813 or 807 (1 μM) were determined by incubation with rHuEPO-α (1 μM) at 37 °C for 1 h in selection buffer, following by 12% non-denatured PAGE at 22 V/cm for 1 h at 4 °C. The gel was stained with ethidium bromide and imaged. All experiments were duplicated.

2.6. Methylation of DNA

Methylation reaction was carried out at 37 °C in 300 μL Tris–HCl (pH 7.4) buffer in the presence of 200 pmol aptamer 807-39nt and 1% dimethylsulfate (DMS) for 1.5 h. The reaction was terminated by the addition of 50 μL solution of 1.5 M acetate sodium and 20 mM 2-mercapto-ethanol, then 1.5-fold cold ethanol was added to precipitate the methylated ssDNA.

2.7. N-deglycosylation of rHuEPO-α

N-glycans were released from rHuEPO-α by enzymatic deglycosylation with PNGase F. After 10 μg rHuEPO-α was added with 4 units of PNGase F to a final volume of 30 μL with 20 mM NH_4HCO_3 at pH 8.0, the reaction was kept at 37 °C for 24 h, and terminated by heating for 5 min at 100 °C. Five microliters reaction solution and 2 μg rHuEPO-α were analyzed by SDS–PAGE. Original and N-deglycosylated rHuEPO-α were mixed with aptamer 807-39nt in selection buffer for 1 h at 37 °C, then applied with EMSA to compare their binding abilities.

2.8. Confocal imaging of cells and tissues bound with aptamer 807-39nt or anti-EPO mAb

The binding behaviors of aptamer 807-39nt to the HLE-B3, T24 cells and clinical tissues were evaluated, respectively. Here antibody AE7A5 was used as the positive control and poly T sequence as the negative control. For the tissues, the paraffin embedded slides of human normal or tumor urothelium were deparaffinized in xylene, rehydrated through graded ethanol, dipped into 10 mM sodium citrate buffer, and treated in a microwave oven at 92–98 °C for 10 min to make antigen retrieval before the experiment. The overnight cultured adherent cells were fixed in absolute methanol at −20 °C for 1 h and washed with phosphate-buffered saline (PBS) before the experiment.

Coverslips with adherent cells or tissue slides were incubated with 100 μL AE7A5 (5 mg/L) or FAM-labeled aptamer 807-39nt (2 μg) in binding buffer containing 5 mM Mg^{2+} for 1 h at 37 °C in the dark. Afterwards the AE7A5 treated tissues or cells were incubated with 1:50 diluted FITC-conjugated goat anti-mouse IgG for 1 h at 37 °C in the dark. After washing with PBS, all the slips were counterstained with 0.25% Evans blue for 15 min to reduce the background of non-specific autofluorescence and to help distinguish the specific FITC or FAM labeling probe from the red background.

The colocalization of aptamer 807-39nt and antibody AE7A5 was performed in T24 cells and urothelium tumor tissues to confirm the binding site of aptamer with cells and tissues. Cells or tissues were incubated with aptamer FITC-807-39nt (2 μg) in selection buffer for 1 h at 37 °C in the dark and then incubated with AE7A5 (0.5 μg) for another 1 h at 37 °C. The slides were then incubated with 1:50 diluted TRITC-conjugated goat anti-mouse IgG for 1 h at 37 °C. After washing with PBS, 4′-6-diamidino-2-phenylindole (DAPI, 100 ng/mL) was adopted to stain the cell nuclei at room temperature for 10 min. The fluorescence patterns of each slide were scanned with a Zeiss LSM 510 META confocal microscope (Zeiss, Germany).

3. Results and discussion

3.1. Isolation of ssDNA aptamers

We designed an affinity chromatographic method special for the whole SELEX procedure, in which an 'affinity tag', lectin, was introduced as a powerful module to attract N-glycans with sialic acid terminal. Using this chromatographic method, we obtained ssDNA aptamers with high affinity and specificity for rHuEPO-α for the first time.

Four factors were considered with regard to this design. Firstly, the structure of rhEPO-α is shown as a left-handed four-helix bundle, the carbohydrate addition sites are clustered at one end of the molecule.[16] Considering the carbohydrates compose ca. 40% of the mass and have an extended and flexible molecular structure, the glycans probably cover most of the molecule surface. Indeed, researches of Toyada et al.[2,17] showed that since many hydrophobic amino acid residues were located at the surface of rhEPO, stabilization of the conformation of intact rhEPO protein was essentially facilitated by the complex-type, especially highly branched N-glycans with extensively stretching hydrophobic groups to provide hydrophobic interactions with the hydrophobic protein surface. Therefore, it was proposed to use lectin as a mediating module to specifically interact with N-glycans, and thus make polypeptide chain moiety be exposed to the oligonucleotide library. Since WGA has a special binding ability for sialic acids and *N*-acetylglucosamines,[18] here WGA-Sepharose acted as the site-selective capturing and releasing module for rHuEPO-α by forming possible target immobilization at certain sites was chosen. Although an alternative approach that would generate aptamers to the peptide moiety of rHuEPO-α is deglycosylation prior to aptamer selection, our developed lectin-mediated affinity selection method is superior and more convenient over the alternative for the easy manipulation, target protein integrity, and native protein conformation preservation.

Secondly, we adopted a structurally constrained library with predefined secondary structure elements which could form a relatively rigid hybridization and leave a large variety of possible shapes from all random sequences for target binding.[19–22] In the iterative in vitro selection process, partially hybridized sequences

in the 5′ and 3′ primers were used to remain invariant for the PCR step. It would deduce the freedoms of unexpected interactions between random sequences and primers, and give a direct pressure towards the evolution of effective random sequences for the target protein.

Thirdly, in order to eliminate the non-specific adsorption, we incubated the oligonucleotide library with WGA-Sepharose in a pre-negative-selection procedure, and improved the stringency of the selection by adding yeast tRNA in each round, enlarging the ratio of ssDNA/rHuEPO-α and increasing the washing times.

Last but not least, a concentration of 5 mM Mg^{2+} was introduced in the selection buffer. Mg^{2+} not only induced advanced structures of the DNA library to facilitate the library–target interaction,[23,24] but also acted as the electrostatic attraction bridge between two negatively charged biomolecules,[25–27] here the two parts were DNA library with phosphodiester backbone and N-glycans with sialylated tetra-antennaries. The important role of Mg^{2+} had been proved as an indispensable aid in binding of an aptameric molecular beacon with rHuEPO-α in our recent article published separately.[28]

The enrichment efficiency was obviously improved after eight rounds of selection. From rounds 1–8, the percentage of bound ssDNAs increased from 15.7% to 65.8%. The selectivity of ssDNAs against rHuEPO-α versus WGA-Sepharose was also increased from 1.4 to 10.6. The band around the marker of 400 base pairs (bp) appeared on the electropherogram was from the main library–target complexes in the EMSA, while the band around 700 bp was another portion of complexes with probably different binding behaviors. With the selection rounds going, the complex band gradually intensified while the band of free library with a faster mobility diminished (Fig. 1).

With an applied pressure in the in vitro selection, the simplest but commonest motif usually survived after selections.[29] Herein to elucidate the selection efficiency of such a structurally constrained library, we sequenced 128 clones from the 6th, 7th, and 8th rounds and traced the exact locations of a certain fragment 'CGAGAT' in the conserved 3′ primer region in the secondary structure level (M-fold simulation[30]). A profit-and-loss relationship was found regarding to the location of the hybridization formed between this fragment and different regions of the sequences for the selection procedure (Table 1). It was shown that of three possible hybridizations, the first two cases (hybridizing entirely with the random sequence or with both the random and primer sequences) appeared less often while the last one (hybridizing solely with 5′ primer region) came out as the dominant type. Thus it was concluded that the CGAGAT fragment interacted preferably with 5′-primer to form

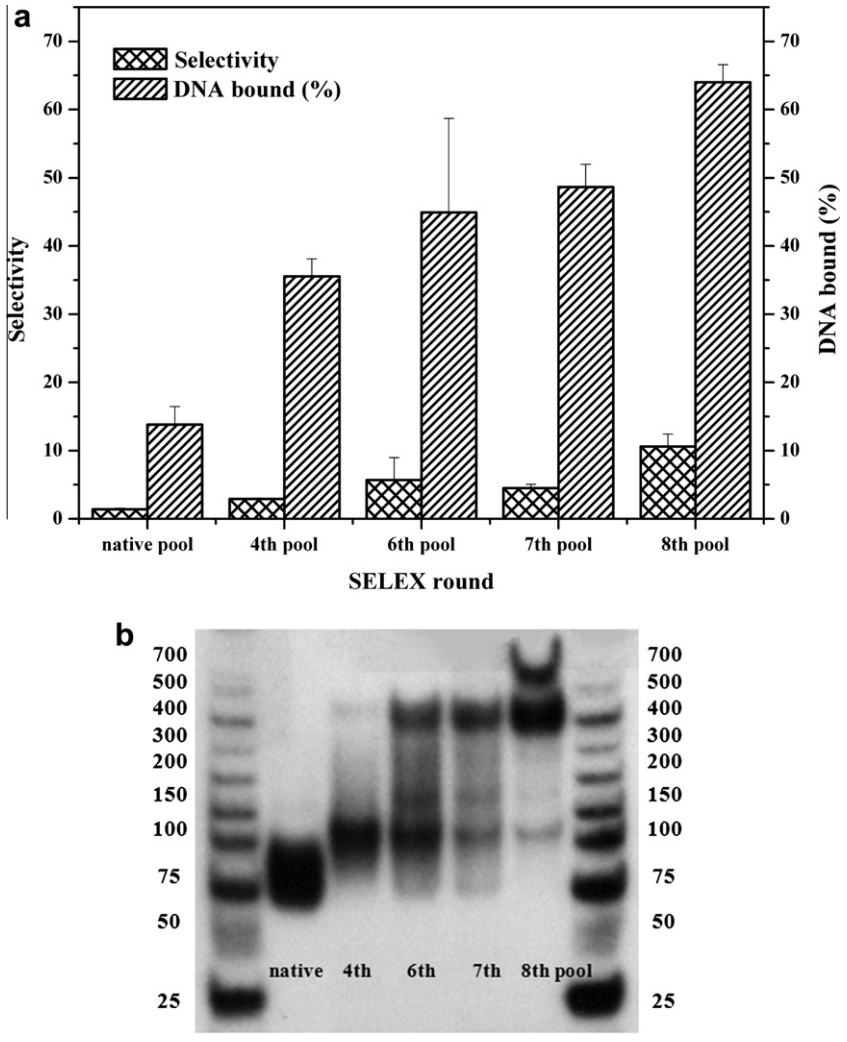

Figure 1. (a) Selectivity and DNA bound percentage of FAM-labeled library (0.5 μM) to rHuEPO-α (2.5 μM) in different SELEX round. Selectivity of ssDNA against rHuEPO-α versus WGA-Sepharose = $FI_{eluent\ of\ sample}/FI_{eluent\ of\ blank}$; the percentage of ssDNA bound = $(FI_{before\ bound} - FI_{after\ bound})/FI_{before\ bound}$; (b) electropherograms of the binding behaviors shown in different rounds of library. The concentration of library and rHuEPO-α in each round is 25 nM and 1 μM, respectively.

Table 1
Different interacted or hybridized locations of CGAGAT fragment in the sequences from 6th to 8th rounds

	Entirely hybridized with random sequences	Interacted with both random and primer sequences			Entirely interacted with primer sequences
		Loop	Stem-loop	Sum	
	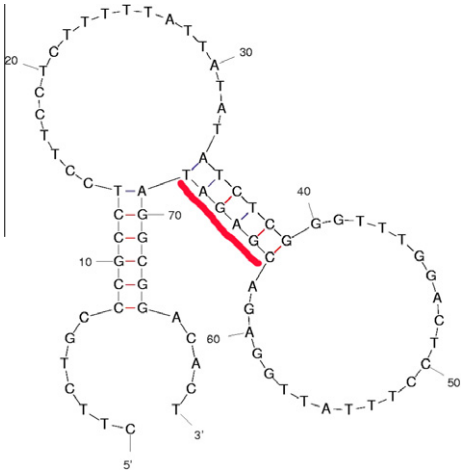	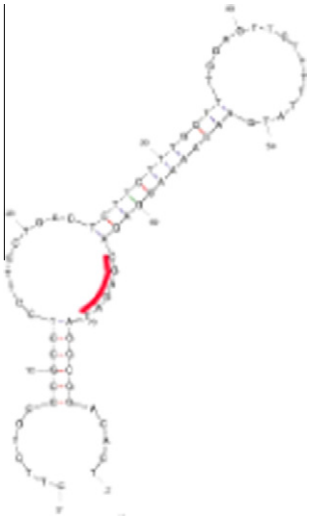	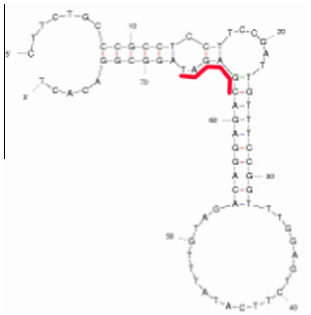		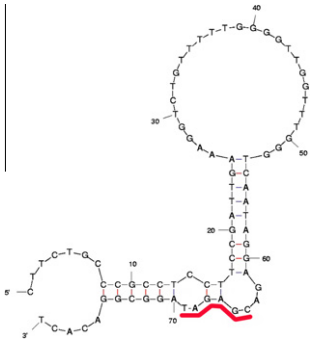
6th	39.5%	4.7%	18.6%	23.3%	11.6%
7th	23.3%	2.3%	7.0%	9.3%	48.8%
8th	2.4%	0%	4.8%	4.8%	64.3%

The line segment shown as 'CGAGAT' fragment in the 3′ primer sequence.

a proper structure accommodation so as to leave the random sequence more freedom to be evolved.

A satisfying enrichment of effective sequences with increasing stringency occurred after all rounds of selection. The finally survived prevalent sequence was aptamer 807, in which CGAGAT fully hybridized with 5′-primer region. It repeated 42 times of all 128 clones with a corresponding percentage of 2.3%, 42%, and 55% in the 6th, 7th, and 8th rounds, respectively. Furthermore, this sequence exhibited by far the highest binding capability for rHuEPO-α.

The homology of all 42 sequences from the 8th round was also analyzed using the online software the MEME Suite. It was found that there were 23 repeated sequences, that is, aptamer 807 in the enriched library and there existed six motifs with not less than eight bases among the different sequences as exhibited in Supplementary Table S2.

3.2. Binding affinity and specificity of some aptamers

Three sequences, 807, 813, and 850, with relative lower Gibbs' free energy of −6.11, −6.16, and −9.28 kcal mol^{-1}, respectively, were selected for K_d value evaluations using EMSA. The K_d values of sequences of 807, 813, and 850 were 82 ± 32 nM, 260 ± 117 nM, and 590 ± 354 nM, respectively (see Supplementary Fig. S1). The specificity of aptamer 807, as an example, was tested by adding 60-fold of other proteins such as HSA, hemoglobin, BSA, lysozyme, and IgG. No protein was observed to have affinity with aptamer 807 (see Supplementary Fig. S2).

Different binding behaviors were arisen from individual aptamer 813 and 807 (see Supplementary Fig. S3). The band of ligand–target complex of aptamer 813 migrated slower than that of aptamer 807. This phenomenon was in accord with that observed in Figure 1b, in which the higher band at the place of ca. 700 bp in EMSA should be mainly attributed by the complex band for EPO and aptamer 813 (and other analogs with same interaction way).

3.3. Truncation of aptamers 813 and 807

Truncation was performed to discriminate the critical sequences for target binding and aptamers 813 and 807 with lower K_d values were studied. Aptamer 813 is shown as a double stem-loop, in which the primer sequence partially hybridized with the random region. According to its secondary structure, aptamer 813 could be truncated as a random sequence with a stem partially hybridized with the primer (813-51nt), then with non-pairs region removed (813-42nt), and finally the random sequence itself (813-40nt). EMSA results showed that aptamer 813-42nt was the shortest motif for binding with rHuEPO-α, and indicated that the stem forming between the random sequence and part of the primer region might facilitate the binding capacity (see Supplementary Fig. S4).

Apatmer 807 was mainly composed of double stem-loops, one formed by the flanking primers and the other by random sequences. Two smaller binding motifs were obtained: 807-68nt (non-pairs region of the primer removed) and 807-39nt (the complete random region). The K_ds of 807, 807-68nt, and 807-39nt gradually decreased in the nM level (Fig. 2), indicating that the recognition between aptamer 807 and rHuEPO-α was dominantly contributed by the random sequence.

3.4. Binding sites of aptamer 807-39nt

Aptamers 807 and 850 belonged to the same family and had similar secondary structures, but they showed different affinity for rHuEPO-α, which suggested some key bases related to specific binding might be present in aptamer 807. The roles of bases located in the stem and loop of aptamer 807-39nt were identified, respectively. A series of stem elongation/shortening/random variation experiments were firstly carried out. It was found that the stem functioned as a support to fix an enclosed loop and stabilize the complex of rHuEPO-α, but had no significant contribution to the specific recognition (Fig. 3).

Further methylation or site-directed mutation towards DNA bases was carried out to single out certain binding sites in the loop of aptamer 807-39nt. Aptamer 807-39nt is composed of a G-rich, T and A bases involved loop and a 5 bp stem. The binding capacity of 807-39nt was lost after methylation (see Supplementary Fig. S5), suggesting that the G and A bases were located within the recognition region.

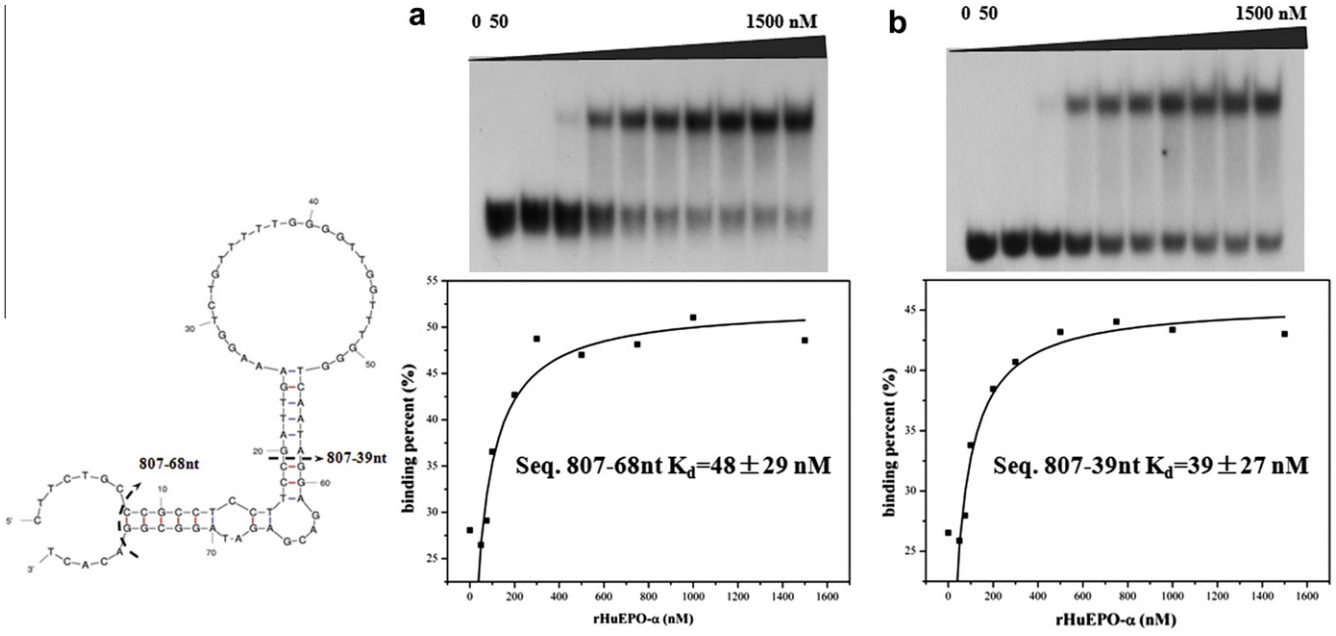

Figure 2. Binding curves of 807-68nt (a); 807-39nt (b) of 25 nM each with increasing concentrations of rHuEPO-α from 0 to 1500 nM in the selection buffer. Top: EMSA of binding behaviors of aptamer and rHuEPO-α; bottom: K_d simulations using one-site binding model.

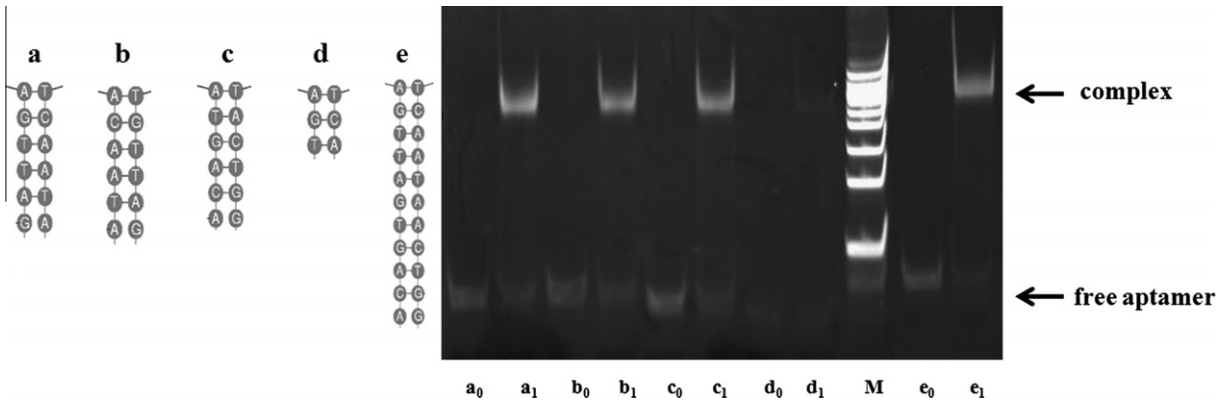

Figure 3. The influence of varied length in the stem of aptamer 807-39nt on its binding behavior with rHuEPO-α in non-denatured PAGE. Lane x_0 and x_1 represent the aptamer analog (1 μM) with or without rHuEPO-α (1 μM), and x represents a, b, c, d, and e, respectively. Lane M represents DNA ladder. (a) Aptamer 807-39nt; (b) the bases of right and left sides are interchanged in the stem of aptamer 807-39nt; (c) the base pairs are randomly substituted; (d) the base pairs are shorten to 3 bp; (e) the base pairs are extended to 11 bp.

Because G-rich loop intended to form advanced tertiary structures, such as G-quartets, it was assumed that the G-rich proportion could be of primary importance for forming the complex. Four pairs of G nucleotides (G_9–G_{10}, G_{22}–G_{23}, G_{26}–G_{27}, and G_{32}–G_{33}) in the loop of 807-39nt were individually replaced by four pairs of C, respectively, and aptamer 807-39nt lost binding capacity after any replacement. A series of single G nucleotide mutation experiments further illustrated that the binding capacity between 807-39nt and rHuEPO-α also vanished when G (G_{10}, G_{22}, G_{27}, and G_{32}) was replaced with C in any of the four locations (Fig. 4).

Additional mutations were performed to the left two A and one C nucleotide in the loop. The replacement of A with T would make the binding capacity of 807-39nt disappear, but changing C to T would not affect the binding (see Supplementary Fig. S6). All above results suggested that G and A were the key binding sites for the complex formation, and varies kinds of non-covalent interaction generated from G and A[31] might contribute to the formation of spatial structure of aptamers 807-39nt when binding with rHuEPO-α.

3.5. Binding moiety of rHuEPO-α with aptamer 807-39nt

Since EPO contained large amount of oligosaccharides, if the sugar chains were the chief binding part between rHuEPO-α and aptamer 807-39nt, the universal application of 807-39nt to other subtype of EPOs might be restricted. We performed deglycosylation experiments to test the most potential binding moiety. PNase F enzyme was employed, which can specifically digested glycans from three N-glycosylation sites at Asn 24, 38, and 83. A di-antennary O-glycan at Ser 126 still remained after treated with PNase F but only reserved ~7% content of all saccharides in rHuEPO-α. In EMSA, the N-deglycosylated rHuEPO-α retained the main binding

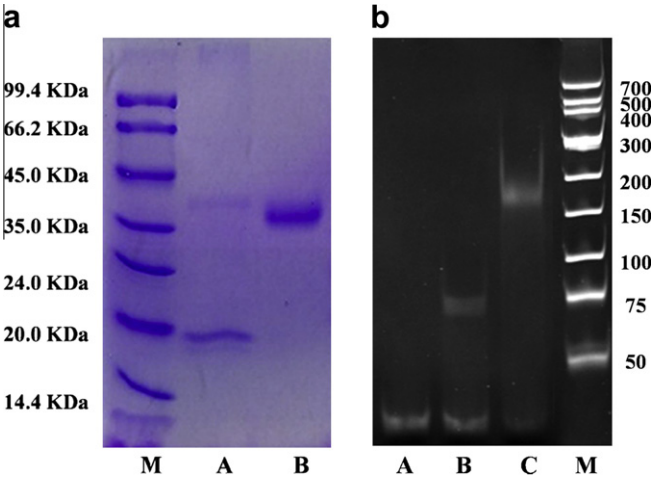

Figure 5. (a) SDS–PAGE of rHuEPO-α before and after deglycosylation. Lanes A and B represent rHuEPO-α with or without PNGase F digestion, respectively. Lane M is protein ladder. (b) Non-denatured PAGE on binding of rHuEPO-α with aptamer 807-39nt (1 μM). Lanes A, B, and C represent aptamer 807-39nt along, aptamer 807-39nt with deglycosylated rHuEPO-α, aptamer 807-39nt with original rHuEPO-α, respectively. Lane M is DNA ladder. The amount of rHuEPO-α before PNGase F treated was identical to intact rHuEPO-α.

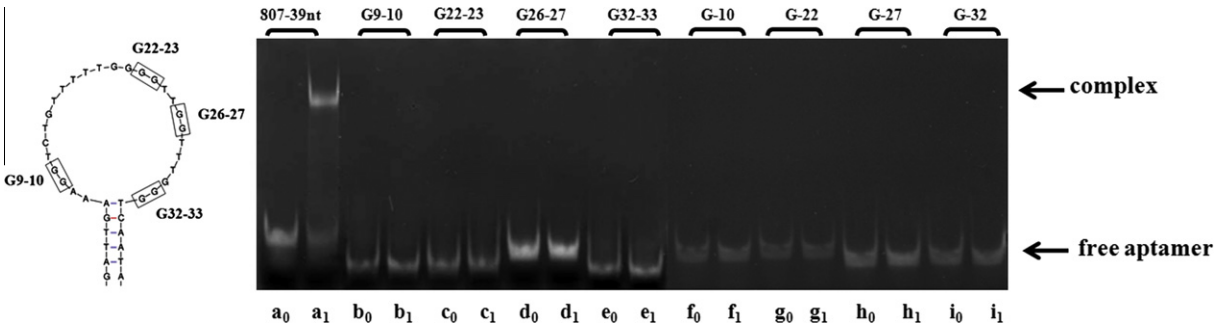

Figure 4. The influence of site-mutation of different G nucleotides in the loop of aptamer 807-39nt on its binding behavior with rHuEPO-α in non-denatured PAGE. Lane x_0 and x_1 represent the aptamer analog (1 μM) with or without rHuEPO-α (1 μM). x represents a, b, c, d, e, f, g, h, and i, respectively. (a) Aptamer 807-39nt only; (b) G_9 and G_{10}; (c) G_{22} and G_{23}; (d) G_{26} and G_{27}; (e) G_{32} and G_{33} in the loop of aptamer 807-39nt are mutated to both C nucleotides, respectively; (f) G_{10}; (g) G_{22}; (h)G_{27}; (i) G_{32} is mutated to C nucleotide in the loop, respectively.

ability with aptamer 807-39nt (Fig. 5). It could be inferred that the peptide chain of rHuEPO-α was of first place in specific binding occurred.

Further proof could be obtained by the binding experiments between aptamer 807-39nt and commercial injection YiBiAo (rHuEPO-α) or Recormn (rHuEPO-β), respectively. rHuEPO-α and rHuEPO-β had the same amino acid sequences but different content of saccharides, and they showed no difference when binding with aptamer 807-39nt (see Supplementary Fig. S7). These results indicated that in the lectin-mediated chromatographic selection method, the polypeptide chain was shown to be the active portion as expected, no additional procedures are needed

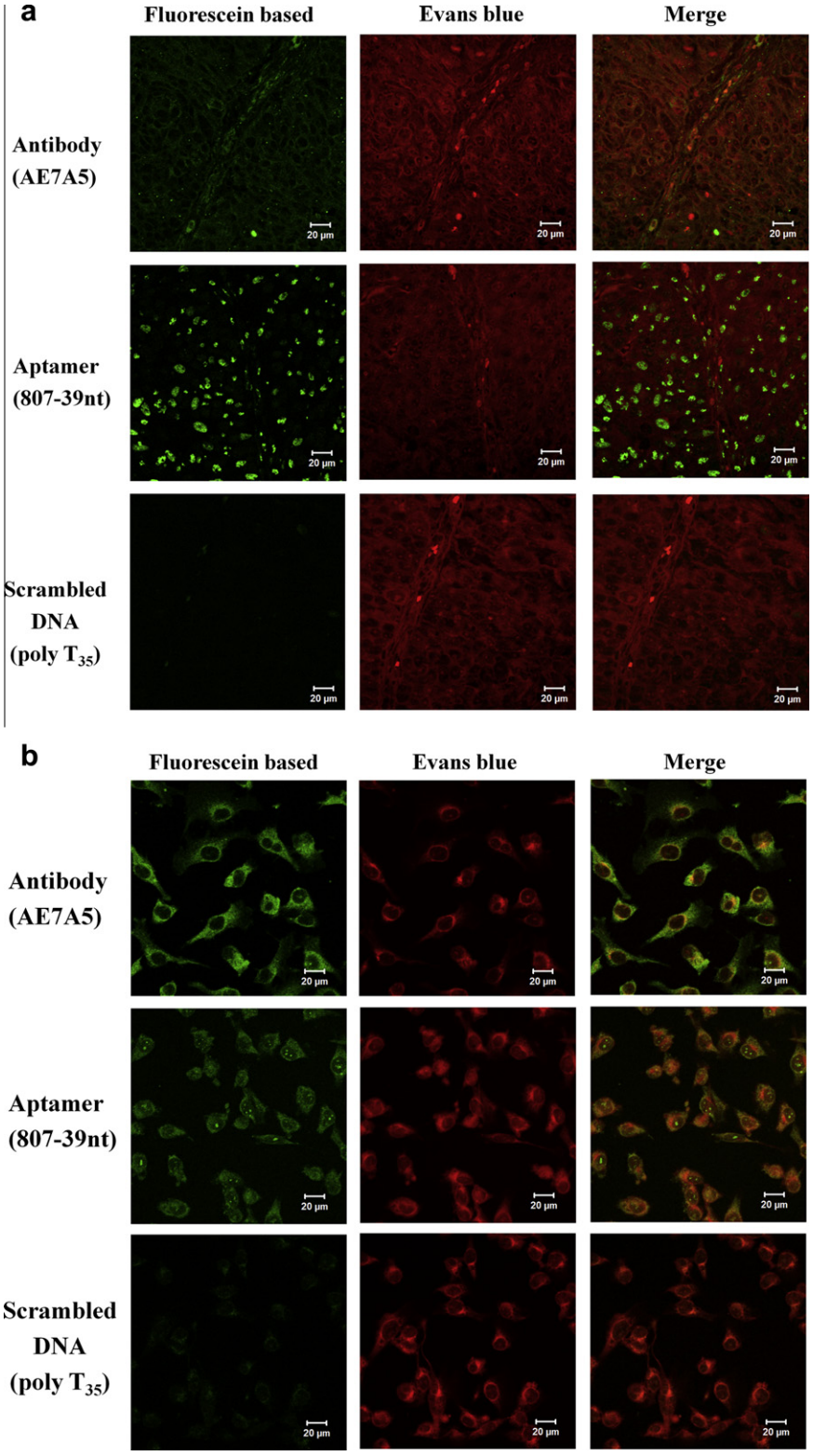

Figure 6. Immuno- and aptameric fluorescence of antibody AE7A5 or aptamer 807-39nt on tumor tissues and cells, poly T here is a negative control. (a) Human malignant tumor urothelium slides; (b) T24 cell adherent cover slips (the scale of the bar is 20 μm).

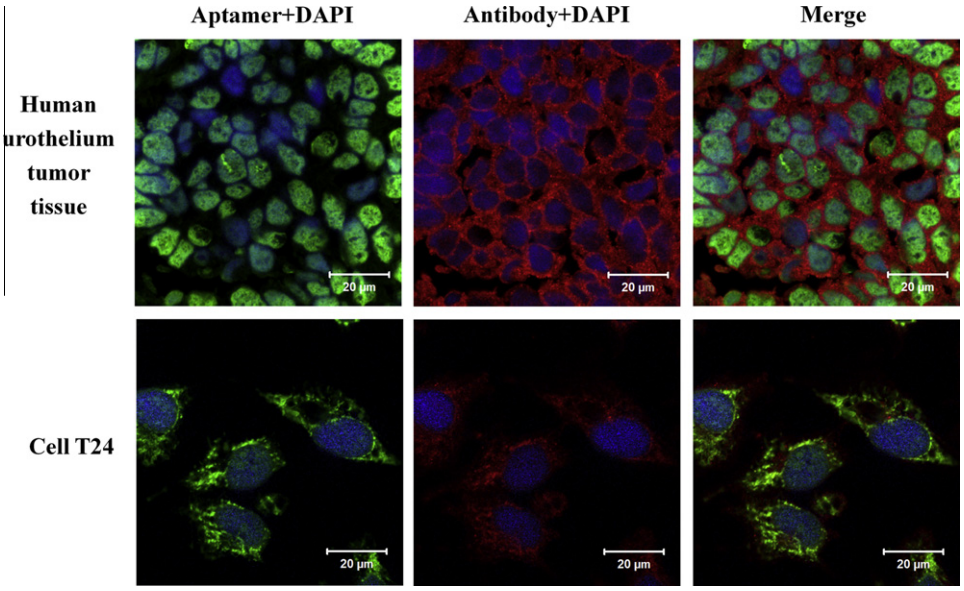

Figure 7. Colocalization of aptamer 807-39nt and antibody AE7A5 in human malignant tumor urothelium sections and T24 cells with confocal microscopy (the scale of the bar is 20 μm).

to remove or separate sugar chains from the polypeptide chain moiety.

3.6. Applications of aptamer 807-39nt

Recent evidence suggested that EPORs had been identified on a variety of primary cancer cells and tumors,[32,33] and investigations usually focused on expression of EPO and EPOR at mRNA and protein level by real time-PCR and immunochemistry due to an autocrine/paracrine mechanism.[34] Here human bladder carcinoma cell line (cell T24) and human tumor urothelium tissue were also tested to verify the binding capacity of aptamer 807-39nt with expressed EPO, normal cell HLE-B3 and normal human urothelium tissues were chosen as the negative controls.

MAb AE7A5 against 26 amino acid residues of EPO N-terminal was widely adopted as the main sensing or capturing molecules in the immunological or mass spectrometric-based analysis, for example, in the World Anti-Doping Agency official method, but it had a broad cross-reactivity with eukaryotic, bacterial proteins, and even human urothelium tissue,[35] which restricted its application in further immunoassays. The confocal imaging results indicated that the aptamer 807-39nt showed less cross-reactivity than mAb AE7A5 in the normal human urothelium paraffin tissue sections (see Supplementary Fig. S8).

The aptameric fluorescence results confirmed that aptamer 807-39nt interacted with the malignant cells and tumor tissues (Fig. 6), whereas negative results of aptamer 807-39nt were observed on normal HLE-B3 cell and normal urothelium tissue slides (see Supplementary Figs. S8 and S9). It was also reported that high amount of overexpressed endogenous EPO existed in epithelial cell oncogenesis,[36,37] implying that the EPO signaling was relevant to the proliferation of tumor cells. Thus aptamer 807-39nt might be used as a new kind of inhibitors to suppress the proliferative activity of tumors.

The colocalization of aptamer 807-39nt and antibody AE7A5 in T24 cells and human tumor urothelium tissues was further investigated by confocal imaging. For tumor cells, aptamer 807-39nt, similar to the antibody, was not only located in cytoplasm, but also in nucleus. For the human tumor urothelium tissues, a clear location shift of aptamer 807-39nt was observed comparing with the case of T24 cells, it exclusively existed in the nucleus (Fig. 7). Different staining patterns of 807-39nt in cultured cells and clinical tissues might be due to the different pretreatment processes of cells and tissues. The tissue slides were more prone to be penetrated for such a small sized aptamer into the nucleus.

4. Conclusions

We have successfully obtained aptamers with high specificity and affinity for glycoprotein rHuEPO-α by a novel WGA lectin-mediated affinity chromatographic SELEX for the first time. Since the hydrophobic surfaces of rHuEPO-α are largely shielded by numerous glycans to provide hydrophobic interactions so as to stabilize the conformation of intact protein, lectin acting as the special binding molecule for sialic acid moiety is chosen in the chromatographic selection, which attributes to a successful SELEX towards certain moiety of peptide chains in rHuEPO-α, and helpful to develop aptamers against 'epotipes' located in the amino acid residues. Binding ability of rHuEPO-α without N-glycosylation moiety for aptamer 807-39nt still remains, which is in agreement with our lectin-mediated SELEX concept.

Typical aptamers have been further characterized. In truncation experiments, for aptamer 813, 813-42nt is the shortest motif for binding with rHuEPO-α, and its secondary structure is a double stem-loop generating from random region and partial primers. For aptamer 807, the affinity of its random sequence (807-39nt) is superior to the full sequence, the stem of 807-39nt acts as the stabilization part and has no contribution to the formation of the complex, while the loop is the key motif for binding with rHuEPO-α. Any nucleotides G and A in the loop of 807-39nt is required for specific binding. Further applications have been executed on the epithelial cancer cell and clinical human urothelium tumor tissues. Positive binding behaviors of aptamer 807-39nt with overexpressed EPO are observed.

In conclusion, aptamer 807-39nt can be regarded as a powerful alternative recognition module for rHuEPO-α, and is expected to be an effective module in the development of new diagnosis methods.

Funding

This work was supported by the National Natural Science Foundation of China [Grants Nos. 20705039 and 30700774] and

National Science and Technology Major Project of the Ministry of Science and Technology of China (Grant No. 2009ZX09301-002).

Conflict of interest statement

None declared.

Acknowledgments

We would also like to thank Professor Ningsheng Shao and Dr. Shaohua Li for helpful discussions in immunohistochemistry experiments.

Supplementary data

Supplementary data associated with this article can be found, in the online version, at doi:10.1016/j.bmc.2010.09.024.

References and notes

1. Skibeli, V.; Nissen-Lie, G.; Peter, T. *Blood* **2001**, *98*, 3626.
2. Toyada, T.; Arakawa, T.; Yamaguchi, H. *J. Biochem.* **2002**, *131*, 511.
3. Choi, D.; Kim, M.; Park, J. *J. Chromatogr., B* **1996**, *687*, 189.
4. Khuri, F. R. *N. Engl. J. Med.* **2007**, *356*, 2445.
5. Weiss, M. J. *Oncologist* **2003**, *8*, 18.
6. Tentori, L.; Graziani, G. *Pharmacol. Res.* **2007**, *55*, 359.
7. Jeong, J. Y.; Feldman, L.; Solar, P.; Szenajch, J.; Sytkowski, A. J. *Int. J. Cancer* **2008**, *122*, 274.
8. Guan, F.; Uboh, C. E.; Soma, L. R.; Birks, E.; Chen, J.; Mitchell, J.; You, Y.; Rudy, J.; Xu, F.; Li, X.; Mbuy, G. *Anal. Chem.* **2007**, *79*, 4627.
9. Ellington, A. D.; Szostak, J. W. *Nature* **1990**, *346*, 818.
10. Tuerk, C.; Gold, L. *Science* **1990**, *249*, 505.
11. Stoltenburg, R.; Reinemann, C.; Strehlitz, B. *Biomol. Eng.* **2007**, *24*, 381.
12. Cao, X.; Li, S.; Chen, L.; Ding, H.; Xu, H.; Huang, Y.; Li, J.; Liu, N.; Cao, W.; Zhu, Y.; Shen, B.; Shao, N. *Nucleic Acids Res.* **2009**, *37*, 4621.
13. Li, S.; Xu, H.; Ding, H.; Huang, Y.; Cao, X.; Yang, G.; Li, J.; Xie, Z.; Meng, Y.; Li, X.; Zhao, Q.; Shen, B.; Shao, N. *J. Pathol.* **2009**, *218*, 327.
14. Berezovski, M. V.; Musheev, M. U.; Drabovich, A. P.; Jitkova, J. V.; Krylov, S. N. *Nat. Protoc.* **2006**, *1*, 1359.
15. Nazarenko, I. In *Fluorescent Energy Transfer Nucleic Acid Probes*; Didenko, V. V., Ed.; Humana Press: NJ, 2006; pp 95–112.
16. Banks, D. D.; Scavezze, J. L.; Siska, C. C. *Biophys. J.* **2009**, *96*, 4221.
17. Toyoda, T.; Itai, T.; Arakawa, T.; Aoki, K. H.; Yamaguchi, H. *J. Biochem.* **2000**, *128*, 731.
18. Fraguas, L. F.; Carlsson, J.; Lönnberg, M. *J. Chromatogr., A* **2008**, *1212*, 82.
19. Hamm, J. *Nucleic Acids Res.* **1996**, *24*, 2220.
20. Davis, J. H.; Szostak, J. W. *Proc. Natl. Acad. Sci. U.S.A.* **2002**, *99*, 11616.
21. Hu, K.; Beck, J.; Nassal, M. *Nucleic Acids Res.* **2004**, *32*, 4377.
22. Biroccio, A.; Hamm, J.; Incitti, I.; de Francesco, R.; Tomei, L. *J. Virol.* **2002**, *76*, 3688.
23. Gokulrangan, G.; Unruh, J. R.; Holub, D. F.; Ingram, B.; Johnson, C. K.; Wilson, G. S. *Anal. Chem.* **2005**, *77*, 1963.
24. André, C.; Xicluna, A.; Guillaume, Y. C. *Electrophoresis* **2005**, *26*, 3247.
25. Sazani, P. L.; Larralde, R.; Szostak, J. W. *J. Am. Chem. Soc.* **2004**, *126*, 8370.
26. Cruz-Aguado, J. A.; Penner, G. *J. Agric. Food Chem.* **2008**, *56*, 10456.
27. Lyubchenko, Y. L.; Shlyakhtenko, L. S. *Proc. Natl. Acad. Sci. U.S.A.* **1997**, *94*, 496.
28. Zhang, Z.; Guo, L.; Tang, J.; Guo, X.; Xie, J. *Talanta* **2009**, *80*, 958.
29. Carothers, J. M.; Szostak, J. W. In *The Aptamers Handbook*; Klussmann, S., Ed.; Wiley-VCH: Weinheim, 2005; pp 7–9.
30. Zuker, M. *Nucleic Acids Res.* **2003**, *31*, 3406.
31. Davis, J. T. *Angew. Chem., Int. Ed.* **2004**, *43*, 668.
32. Yasuda, Y.; Fujita, Y.; Matsuo, T.; Koinuma, S.; Hara, S.; Tazaki, A.; Onozaki, M.; Hashimoto, M.; Musha, T.; Ogawa, K.; Fujita, H.; Nakamura, Y.; Shiozaki, H.; Utsumi, H. *Carcinogenesis* **2003**, *24*, 1021.
33. Hardee, M. E.; Arcasoy, M. O.; Blackwell, K. L.; Kirkpatrick, J. P.; Dewhirst, M. W. *Clin. Cancer Res.* **2006**, *12*, 332.
34. Jeong, J. Y.; Hoxhaj, G.; Socha, A. L.; Sytkowski, A. J.; Feldman, L. *Mol. Cancer Res.* **2009**, *7*, 1150.
35. Franke, W. W.; Heid, H. *Clin. Chim. Acta* **2006**, *373*, 189.
36. Fandrey, J.; Dicato, M. *Oncologist* **2009**, *14*, 34.
37. Chabowska, A. M.; Sulkowska, M.; Chabowski, A.; Wincewicz, A.; Koda, M. *Int. J. Surg. Pathol.* **2008**, *16*, 269.